Binary Blends of Polyethers with Fatty Acids: A Thermal Characterization of the Phase Transitions

Krzysztof Pielichowski, Kinga Flejtuch

Department of Chemistry and Technology of Polymers, Technical University, ul. Warszawiska 24, 31-155 Kraków, Poland

Received 4 December 2002; accepted 8 January 2003

ABSTRACT: A series of binary blends of poly(ethylene oxide) (PEO), poly(propylene oxide) (PPO), and polytetrahydrofuran (PTHF), characterized by similar average molecular weights, with selected fatty acids (capric acid, lauric acid, myristic acid, palmitic acid, and stearic acid) were prepared by melt mixing. Differential scanning calorimetry was applied to characterize the phase transitions of melting and crystallization, and a synergistic effect was found to occur for PEO/fatty acid blends, as evidenced by the values of the enthalpy of the phase transition. This effect was probably due to hydrogen bonding between PEO and the fatty (carboxylic) acids, which facilitated the formation of crystalline structures; an analysis of IR spectroscopy data showed a shift in the absorption bands of OH groups. The morphology development of the PEO/carboxylic acid blends, as observed with polarizing light microscopy, could be described as spherulitic growth with spontaneous selection of the lamellar thickness. The textures of the individual fibrils, consisting of stacks of several tens of lamellae corresponding to PPO and PTHF, were less regular than the texture of PEO and showed large macroscopic heterogeneity.
 J Appl Polym Sci 90: 861–870, 2003

Key words: polyethers; crystallization; morphology; differential scanning calorimetry (DSC)

INTRODUCTION

Polyethers, such as poly(ethylene oxide) (PEO), poly(propylene oxide) (PPO), and polytetrahydrofuran (PTHF), are important materials for medicine, bioengineering, and green-chemical industries.[1,2] Processing is usually performed in the molten state, just over the melting temperature; if the temperature drops, crystallization occurs, its rate being governed by the thermodynamic driving force (entropy factor) and mobility of the polymer chain (diffusion factor).[3] Depending on the conditions, crystal nucleation is the first step of any crystallization, but it can be avoided by incomplete melting before crystallization (self-nucleation). Molecular nucleation, in contrast, can only be affected by changes in the molecular conformation in the melt (e.g., by the presence of a second substance).[4]

This issue is related to the novel and promising applications of polyethers for thermal energy storage; organic phase-change materials (PCMs) do not show phase separation, are essentially nontoxic, stable, and noncorrosive, and have high flash points.[5,6] The explanation for the applicability of PEO, for example, as a PCM material lies in its structure: PEO is arranged as lamellae, with the chains existing in either extended or folded forms, the latter being metastable with respect to the extended-chain conformation. One should, however, be aware that the crystallization of polymers from metastable liquids is a complex issue because of their topological connectivity: the ability of different portions of a single polymer molecule to participate in different initial nuclei is associated with entropic frustration and leads to incomplete crystallization, by which polymer chains fold back and forth to form crystalline lamellae.[7] The free energy of a folded state results from attractions among nonbonded monomers and penalties for torsional bending along the chain backbone. Different folded states of the crystalline polymer have different free energies and must be separated by barriers that are responsible for the spontaneous selection of the lamellar thickness.[8]

Parallel fatty acids have a relatively high latent heating and exhibit small volume changes during the phase transition. Because both classes of substances are compatible and can easily be blended and processed by melt mixing, we decided to study the phase transitions of selected polyether/fatty acid blends by differential scanning calorimetry (DSC) for their further consideration as novel and efficient thermal energy storage materials.

EXPERIMENTAL

Materials

PEO with an average molecular weight of 3400, PPO with an average molecular weight of 4000, PTHF with an

Correspondence to: K. Pielichowski (kpielich@usk.pk.edu.pl).
Contract grant sponsor: Polish Committee for Scientific Research; contract grant number: PB 0975/T09/2002/22.

TABLE I
Thermal Characterization of the Phase Transitions of Polyethers

	Melting				Freezing		
Sample	Melting range (°C)	Melting point (°C)	Heat of melting (J/g)	X_c (%)	Freezing range (°C)	Freezing point (°C)	Heat of crystallization (J/g)
PEO	51.9–65.2	63.4	166.8	84.7	30.4–39.0	36.7	158.3
PPO	−11.5 to 6.0	−9.2	0.6	0.4	—	—	—
PTHF	23.9–33.7	29.7	91.0	45.5	−3.8 to 5.7	0.2	85.4

average molecular weight of 2900, and fatty acids [capric acid ($C_9H_{19}COOH$), lauric acid ($C_{11}H_{23}COOH$), myristic acid ($C_{13}H_{27}COOH$), palmitic acid ($C_{15}H_{31}COOH$), and stearic acid ($C_{17}H_{35}COOH$)] were acquired from Aldrich Chemical Co. (Steinheim, Germany).

The results of the thermal characterization of the phase transitions of the polyethers and carboxylic acids used in this study are collected in Tables I and II. A description of the binary polyether/fatty acid blends is presented in table III.

Techniques

Differential scanning calorimetry (DSC)

For the DSC measurements, a Netzsch DSC 200, operating in a dynamic mode, was employed. Each sample (ca. 5 mg) was placed in a sealed aluminum pan. A heating/cooling rate of 10 K/min was applied. Argon was used as an inert gas at a flow rate of 30 cm^3/min. Before being used, the calorimeter was calibrated with mercury and indium standards; an empty aluminum pan was used as a reference. Liquid nitrogen was used as a cooling medium.

Polarized light microscopy (PLM)

Microscopic investigations were performed with a light polarizing microscope with a vision track (PZO, Warsaw, Poland). Each sample was put on a glass plate, and a series of pictures was taken during the crystallization process.

TABLE II
Thermal Characterization of the Phase Transitions of Carboxylic Acids

Sample	Melting point (°C)	Heat of melting (J/g)	Freezing point (°C)	Heat of crystallization (J/g)
Capric acid	35.6	169.9	24.7	170.3
Lauric acid	48.5	187.7	37.1	187.2
Myristic acid	61.0	201.0	45.9	201.0
Palmitic acid	66.8	216.5	53.5	218.1
Stearic acid	72.5	220.4	60.5	221.1

Fourier transform infrared (FTIR) spectroscopy

IR spectra of the samples (KBr pellets) were recorded on a Bio-Rad FTS 165 FTIR spectrometer at a resolution of 4 cm^{-1}.

RESULTS AND DISCUSSION

PEO shows a higher enthalpy of melting and crystallization than PPO and PTHF.

PEO is arranged as lamellae, with the chains existing in either extended or folded forms, the latter being metastable with respect to the extended-chain conformation. The crystallization behavior and microstructural development of PEO were investigated by Lisowski et al.,[9] who performed a series of time-resolved synchrotron wide-angle and small-angle X-ray scattering experiments. The values of n* for the dominant first process (encompassing the first 60–70% of the crystallization process) have been found to be between 2 and 3 (roughly consistent with the expectation of spherulite formation), whereas those of the second

*According to the Avrami expression, $1 - X_c = \exp(-zt^n)$, where X_c is the fraction crystallized at time t ($X_c = 1$ at the end of crystallization), z is a constant dependent on nucleation and growth rates, and n is related to the type of nucleation and growth geometry.

TABLE III
Description of the Binary Polyether/Fatty Acid Blends

Sample	Polymer/fatty acids blend (1:1 w/w)
1	PEO/capric acid
2	PEO/lauric acid
3	PEO/myristic acid
4	PEO/palmitic acid
5	PEO/stearic acid
6	PPO/capric acid
7	PPO/lauric acid
8	PPO/myristic acid
9	PPO/palmitic acid
10	PPO/stearic acid
11	PTHF/capric acid
12	PTHF/lauric acid
13	PTHF/myristic acid
14	PTHF/palmitic acid
15	PTHF/stearic acid

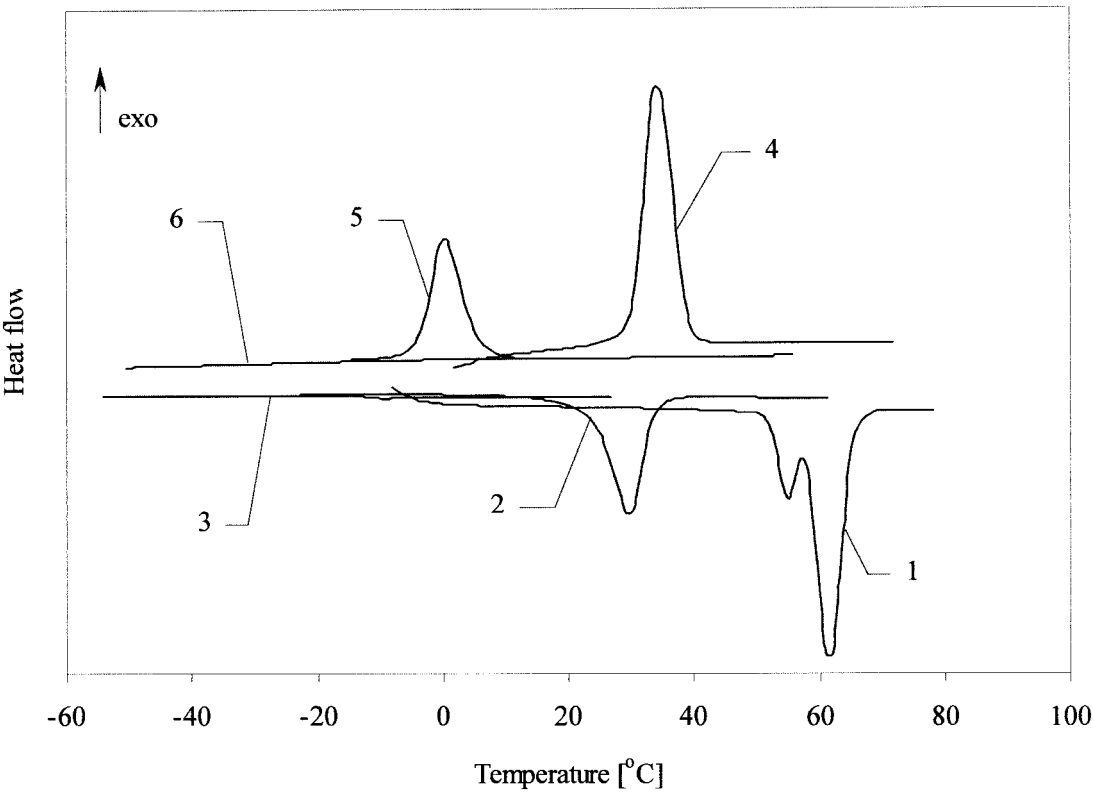

Figure 1 DSC profiles of PEO, PPO, and PTHF: (1) PEO (melting), (2) PTHF (melting), (3) PPO (melting), (4) PEO (freezing), (5) PTHF (freezing), and (6) PPO (freezing).

process are near 1. The obtained values are similar to those reported previously in a DSC study of a binary mixture of low- and high-molecular-weight PEO fractions,[10] and it was suggested that molecular segregation of the lower molecular weight species was responsible for the longer time process. A value of $n \sim 1$ for the second process has been associated with rodlike growth nucleated on existing crystal surfaces.[11] The results of real-time wide-angle X-ray diffraction/small-angle X-ray scattering melting experiments pointed to lamellar insertion within or between lamellar stacks as morphology development during crystallization.

PPO in its atactic stereoregular form is an amorphous polymer; the presence of methyl substituents substantially hinders the formation of hydrogen bonds and subsequent crystallization.

PTHF displays properties between those of PEO and PPO; there are no spatial constraints in the form of a substituent, but there is a longer space between oxygen atoms in the macromolecular chain, and so the hydrogen bonding is not as strong as for PEO. DSC

TABLE IV
Parameters of the Phase Transitions of Binary Blends of PEO with Fatty Acids Obtained by DSC

	Melting			Freezing		
Sample	Melting range (°C)	Melting point (°C)	Heat of melting (J/g)	Freezing range (°C)	Freezing point (°C)	Heat of crystallization (J/g)
PEO/capric acid	28.0–44.9	32.2 42.0	169.1	12.8–17.4	15.2	159.1
PEO/lauric acid	42.6–54.2	47.1	188.3	24.0–35.3	28.1 32.5	178.3
PEO/myristic acid	45.0–58.3	50.7 54.9	207.3	24.6–45.3	27.1 42.6	195.1
PEO/palmitic acid	45.3–64.4	51.2 58.0	209.0	25.4–52.9	29.9 49.7	201.2
PEO/stearic acid	49.9–72.1	54.2 60.3 68.9	204.9	30.5–62.5	33.7 60.3	201.9

TABLE V
Parameters of the Phase Transitions of Binary Blends of PPO with Fatty Acids Obtained by DSC

	Melting			Freezing		
Sample	Melting range (°C)	Melting point (°C)	Heat of melting (J/g)	Freezing range (°C)	Freezing point (°C)	Heat of crystallization (J/g)
PPO/capric acid	18.7–32.1	28.3	95.3	7.6–20.0	13.8 17.9	88.3
PPO/lauric acid	30.9–43.7	40.2	100.5	24.4–32.7	29.6	82.0
PPO/myristic acid	41.2–54.8	51.5	100.0	34.9–44.0	40.8	94.8
PPO/palmitic acid	47.6–63.7	60.0	93.9	39.6–52.2	48.6	94.8
PPO/stearic acid	57.1–69.0	66.0	107.9	49.5–58.8	56.3	105.9

profiles of PEO, PPO, and PTHF, showing the melting and crystallization behavior, are presented in Figure 1.

The physical properties of the carboxylic acids reflect the strong hydrogen bonding between carboxylic acid molecules. The melting points and boiling points are relatively high;[12,13] the saturated fatty acids exhibit small volume changes during the phase transition and little or no supercooling during freezing.

The DSC results for binary blends of PEO, PPO, and PTHF with the fatty acids are collected in Tables IV–VI.

In all of the blends, a broadening of the temperature range can be observed in comparison with the phase transitions of pure components, along with a temperature shift toward lower values. For PEO and PTHF blends, DSC curves display peaks that originate from both the polymer and acid; for PPO blends, only acid peaks can be observed. The freezing of blends takes place over a broader temperature range than for melting because of a supercooling effect (Figs. 2–4).

For the blends under investigation, the theoretical values of the heats of the phase transition have been calculated:

$$\Delta H_b = \Delta H_p x_p + \Delta H_a x_a$$

where ΔH_b is the heat of phase transition of the blend; ΔH_p is the heat of phase transition of the polymer; ΔH_a is the heat of phase transition of the acid; and x_p and x_a are the weight fractions of the polymer and acid, respectively. The results are presented in Figures 5 and 6.

For the PEO blends, the experimental values are higher than expected from the theoretical calculations. This is probably due to the facilitated formation of hydrogen bonding between the hydrogen atom from the carboxylic group in acid molecules and the ether oxygen from the poly(oxyethylene) chain, which, in turn, enhances the formation of crystalline structures (lamellae).

To gain more detailed insight into the structures of the blends, we performed FTIR measurements of pure PEO, lauric acid, and a PEO/lauric acid (1:1 w/w) blend (Figs. 7–9).

An analysis of the FTIR spectra reveals that lauric acid is in a dimer form (—C═O stretching, 1704 cm^{-1}) and that no esterification reaction between PEO hydroxyl groups and carboxylic groups from the acid takes place. The self-association of PEO is evidenced by an absorption band at 3449 cm^{-1} (—OH stretching), which, for the blend, is shifted by about 30 cm^{-1} toward a lower wave number. This frequency difference can be considered a measure of the average strength of the intermolecular hydrogen bonding.[14,15] However, the peak of the —C═O absorption band

TABLE VI
Parameters of the Phase Transitions of Binary Blends of PHTF with Fatty Acids Obtained by DSC

	Melting			Freezing		
Sample	Melting range (°C)	Melting point (°C)	Heat of melting (J/g)	Freezing range (°C)	Freezing poing (°C)	Heat of crystallization (J/g)
PTHF/capric acid	12.5–29.4	18.0	137.1	−5.3–14.9	−1.4 11.7	128.1
PTHF/lauric acid	18.9–41.5	23.3 38.3	140.6	−0.5–29.8	6.1 27.5	134.0
PTHF/myristic acid	22.3–53.3	26.1 50.4	146.4	4.6–42.7	8.8 40.1	138.3
PTHF/palmitic acid	21.5–61.0	26.0 57.9	149.3	4.0–50.4	8.5 47.6	151.0
PTHF/stearic acid	21.9–68.2	26.5 65.1	151.6	4.5–57.7	8.2 55.4	156.4

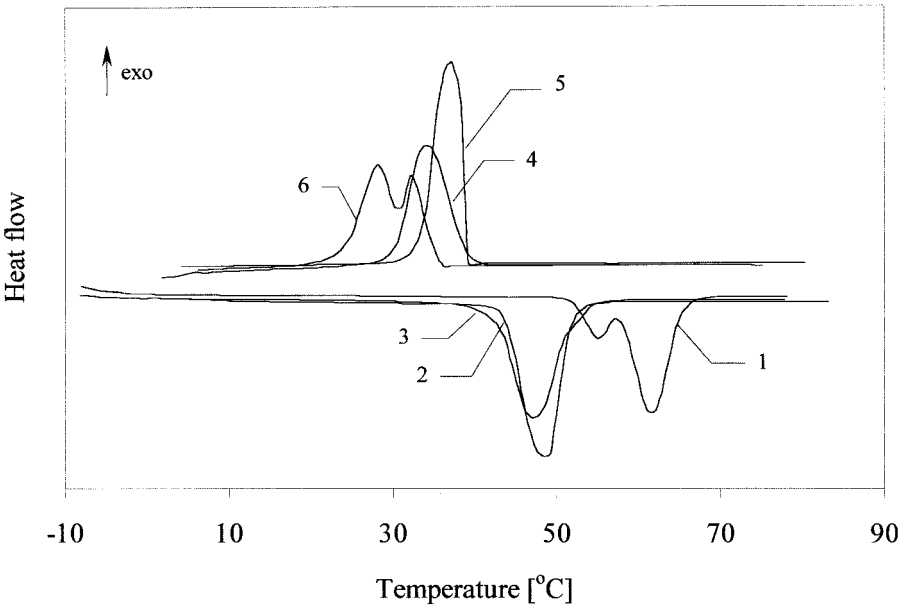

Figure 2 DSC profiles of PEO, lauric acid, and a PEO/lauric acid blend: (1) PEO (melting), (2) pure lauric acid (melting), (3) PEO/lauric acid (melting), (4) PEO (freezing), (5) pure lauric acid (freezing), and (6) PEO/lauric acid (freezing).

remains unaffected, although the shoulder has a different shape. The self-association of PEO in carbon tetrachloride was studied by Phillipova et al.,[16] who obtained equilibrium constants for the interactions between the hydroxyl end groups and the ether groups of the main chain. Haynes et al.[17] experimentally examined aqueous solutions of PEO and dextran; Polik and Burchard[18] found, using static light scattering, that PEO forms large aggregates in solution. Economou et al.[19] studied hydrogen bonding between polymers and solvents that could both self-associate and solvate as well as compounds that could only solvate with FTIR; the spectra were analyzed with derivatives and Fourier self-deconvolution to establish the numbers and positions of the peaks, which were than subjected to profile modeling. According to the authors, potential problems are connected to the distortion of the derivative if a boxcar truncation technique eliminates an important part of the spectrum in addition to the noise. The complexation of PEO with urea

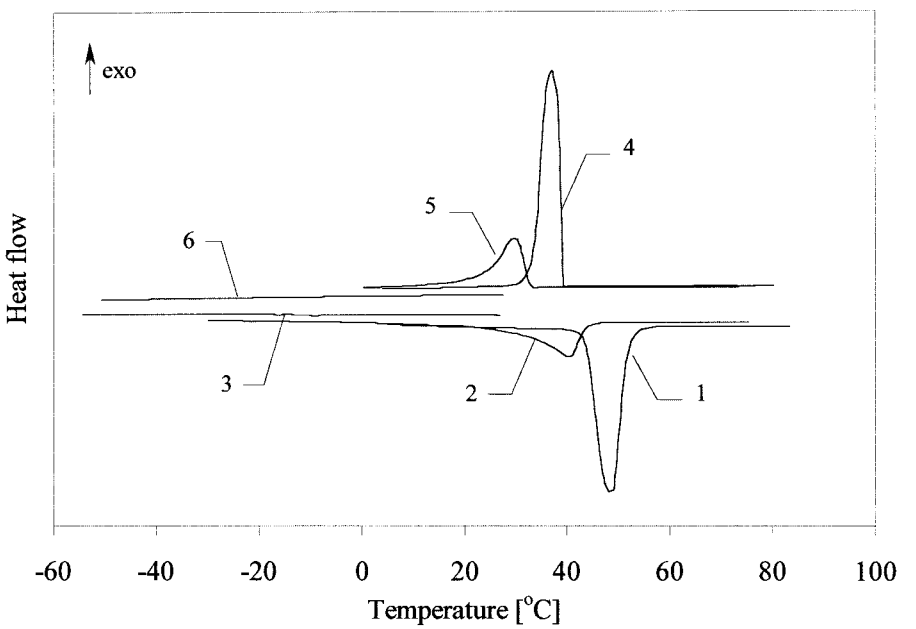

Figure 3 DSC profiles of PPO, lauric acid, and a PPO/lauric acid blend: (1) pure lauric acid (melting), (2) PPO/lauric acid (melting), (3) PPO (melting), (4) pure lauric acid (freezing), (5) PPO/lauric acid (freezing), and (6) PPO (freezing).

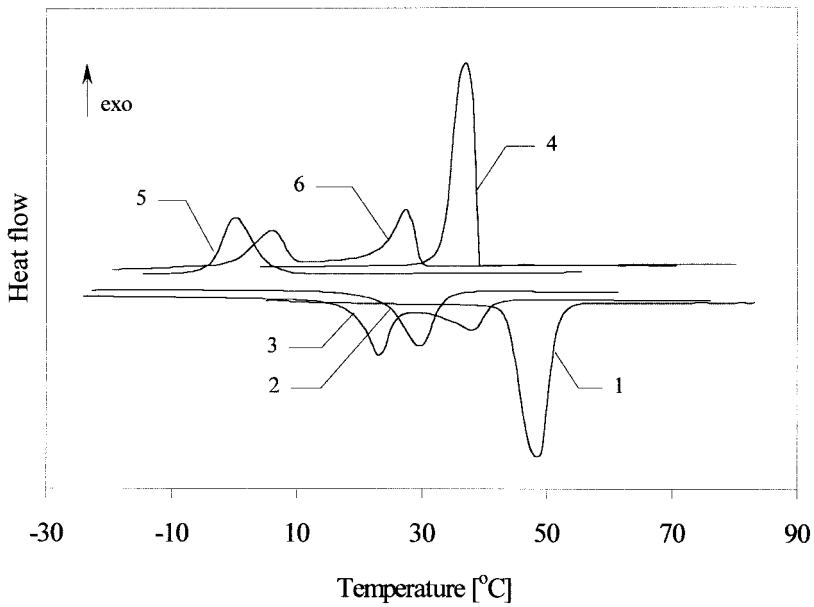

Figure 4 DSC profiles of PTHF, lauric acid, and a PTHF/lauric acid blend: (1) pure lauric acid (melting), (2) PTHF (melting), (3) PTHF/lauric acid (melting), (4) pure lauric acid (freezing), (5) PTHF (freezing), and (6) PTHF/lauric acid (freezing).

in both solid and molten states was studied with IR by Bogdanov et al.[20] The formation of a high-temperature, metastable molecular complex was confirmed spectroscopically. In an another work, Rego et al.[21] analyzed hydrogen bonding in poly(*N*-vinyl pyrrolidone)/poly(monobenzyl itaconate) blends in which the unperturbed positions and absorbances of the poly(monobenzyl itaconate)carbonyl vibrations indicated that the possible source of self-association in this polyether might arise from interactions between the acidic hydroxyl group and the ether oxygen atom, the basicity of the latter being enhanced by the presence of the aromatic ring; at the same time, the position of the poly(monobenzyl itaconate) C═O vibration bands remained unaffected.

The phase behavior of poly(ethylene-*co*-methacrylic acid)/polyether blends (containing a strongly self-associated polymer in which the formation of intermolecular hydrogen-bonded dimers occurs exclusively rather than chainlike structures) has been studied by DSC and FTIR methods.[22] Authors have developed a theoretical model based on Flory–Huggins equation that takes into account the intermediate complexes as distinguishable species and allows these to randomly mix. The change in the distribution of these species with the concentration can be accounted for by the correct choice of the reference state; the equilibrium constants are a measure of the change in free energy per hydrogen bond.

It has already been observed that chains of PEO integrally fold when incorporated into crystals, as evidenced by quantified changes of the lamellar thickness under various crystallization conditions.[23,24] Cheng and coworkers investigated the crystallization behavior of PEO with different average molecular weights and applied nucleation theory to analyze the extended-chain crystal growth of low-molecular-mass PEO fractions at low supercoolings. To obtain the slope of the relationship between G (the crystal growth rate) and ΔT (supercooling) in the form of the K value in regime I[†], they applied different values of σ' (the transient surface free energy associated with the two chain-end-type surfaces exposed to the melt).[25] The reason is recognized in the experimental observations of different self-diffusion coefficients and melt viscosities.[26] This phenomenon has been attributed to an end-group effect because low-molecular-mass PEO fractions can form hydrogen bonding not only in the solid state but also in the melt.[27] This association in the melt may lead to increasingly rough chain-end crystal surfaces, which involve some kinetic ciliation.[28] In our study, we have observed that there

[†]The kinetic nucleation theory has emerged as a promising framework for describing and understanding isothermal crystallization rates for linear polymers in quiescent melts or dilute solutions.[29,30] There are three regimes of crystal growth that are controlled by competing nucleation and growth processes. The first regime (I) describes a single nucleation per substrate length L, where the nucleation rate i is slower than the substrate completion rate g. The crystal growth rate is given by $G_I = biL$, where b is the thickness of a crystalline stem. In the second regime (II), multiple nucleation occurs on the growth face as the nucleation rate is roughly equivalent to or greater than the substrate completion rate. The crystal growth rate is given by $G_{II} = b(2ig)^{1/2}$. The final regime (III) is a state of rapid polynucleation growth in which nucleation occurs so rapidly that the separation of niches on the substrate that characterizes regime II approaches the width of a single stem.[31]

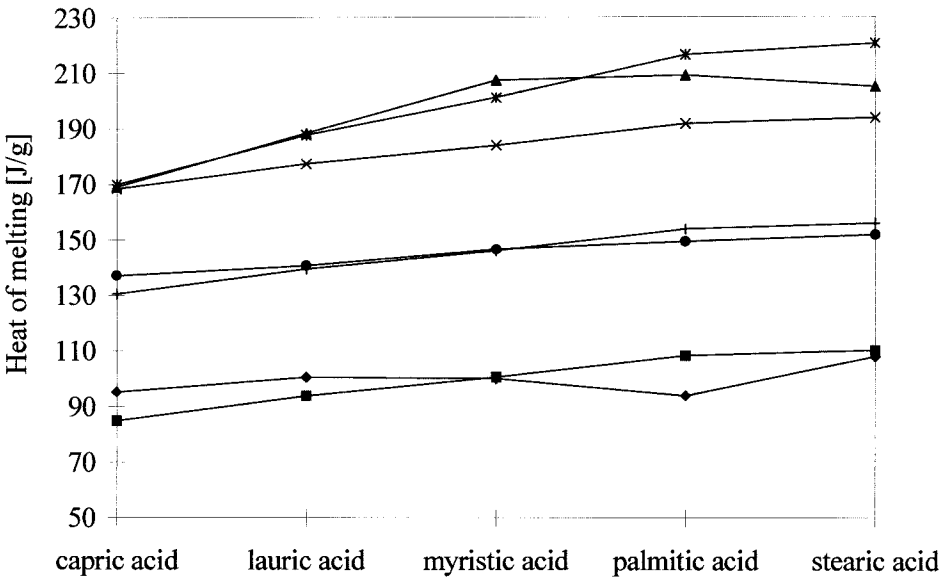

Figure 5 Theoretical and experimental values of the heats of melting for polyether/fatty acid blends: (♦) PPO/fatty acid (experimental), (■) PPO/fatty acid (theoretical), (●) PTHF/fatty acid (experimental), (+) PTHF/fatty acid (theoretical), (▲) PEO/fatty acid (experimental), (×) PEO/fatty acid (theoretical), and (*) pure fatty acid.

are considerable differences in the morphology development of PEO, PTHF, and PPO blends (Figs. 10–12).

A regular formation of lamellae directly on the surface can be seen for the PEO blend, whereby for the PTHF and PPO blends, irregular interfacial semicrystalline structures are observed that lower the overall degree of crystallinity. The textures of the individual fibrils, consisting of stacks of several tens of lamellae corresponding to PPO and PTHF, are less regular than the texture of PEO (in which aggregates of interconnected cup-shaped lamellae and relatively tightly packed structures of twisted lamellae have been observed) and show large macroscopic heterogeneity. In addition, some features of epitaxial growth of folded-chain lamellae that are close together or interlocked can be observed.

The melting of PEO with an average molecular weight of 1500 or 4500, studied with temperature-modulated DSC, was found to be practically completely irreversible for sufficiently well-crystallized, long-chain molecules.[32] A quasi-isothermal analysis of the melting process was taken as proof that molecular

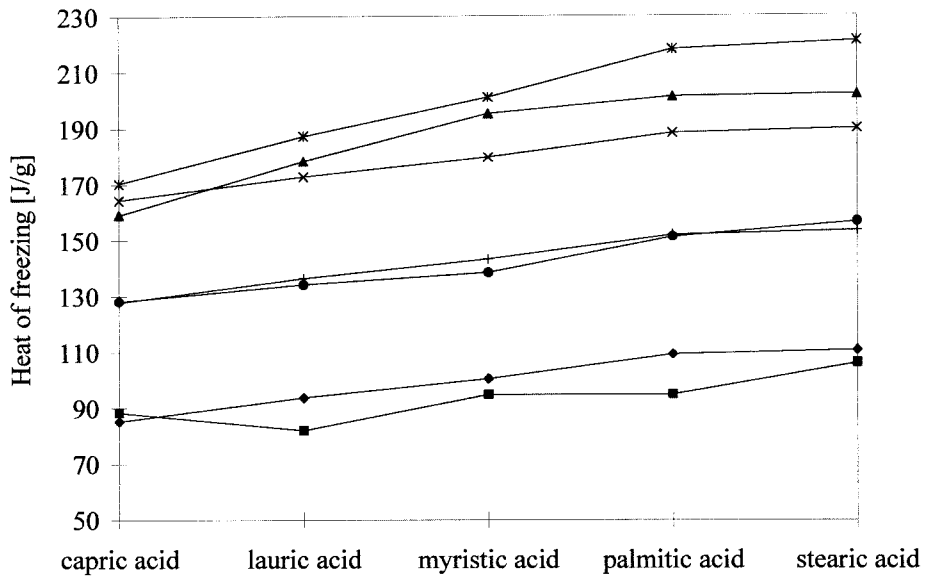

Figure 6 Theoretical and experimental values of the heats of freezing for polyether/fatty acid blends: (♦) PPO/fatty acid (experimental), (■) PPO/fatty acid (theoretical), (●) PTHF/fatty acid (experimental), (+) PTHF/fatty acid (theoretical), (▲) PEO/fatty acid (experimental), (×) PEO/fatty acid (theoretical), and (*) pure fatty acid.

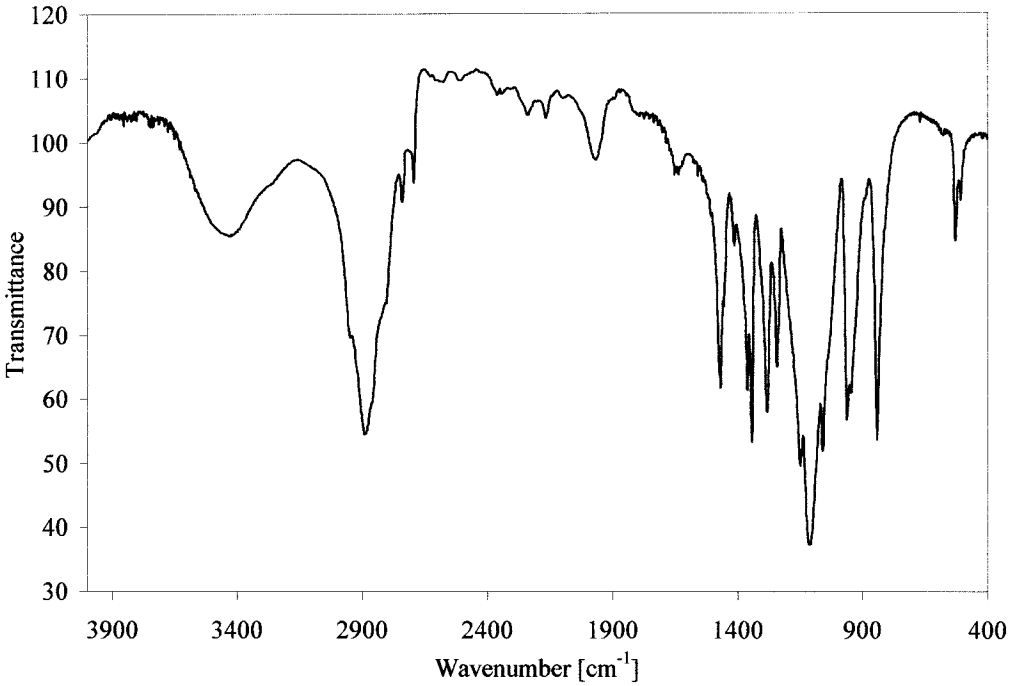

Figure 7 FTIR spectrum of PEO.

nucleation—a rate-determining step with a free-enthalpy barrier for the beginning of crystallization of a molecule or, at a higher supercooling, a part of a molecule on the surface of a crystal—is needed in addition to crystal nucleation.

Similar crystal structures of PEO under the external force of an electric field were detected by Park and Robertson.[33] Because PEO belongs to polymers with permanent dipoles or high dielectric constants, electric fields have often been employed to create anisotropic

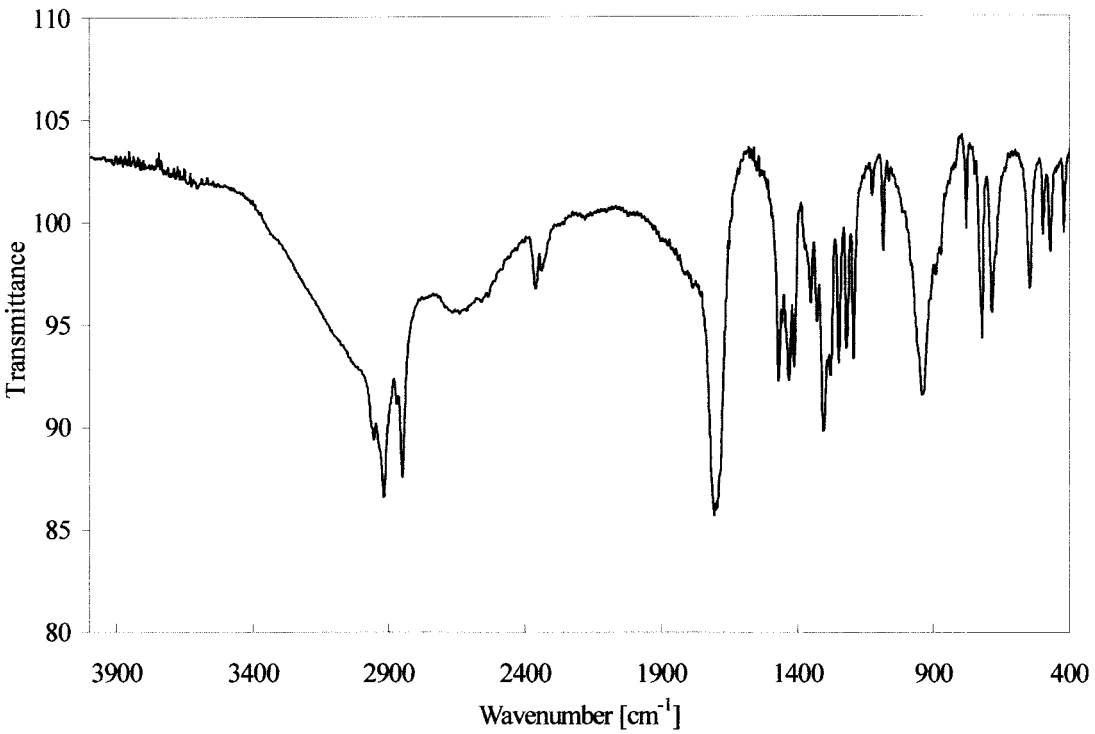

Figure 8 FTIR spectrum of lauric acid.

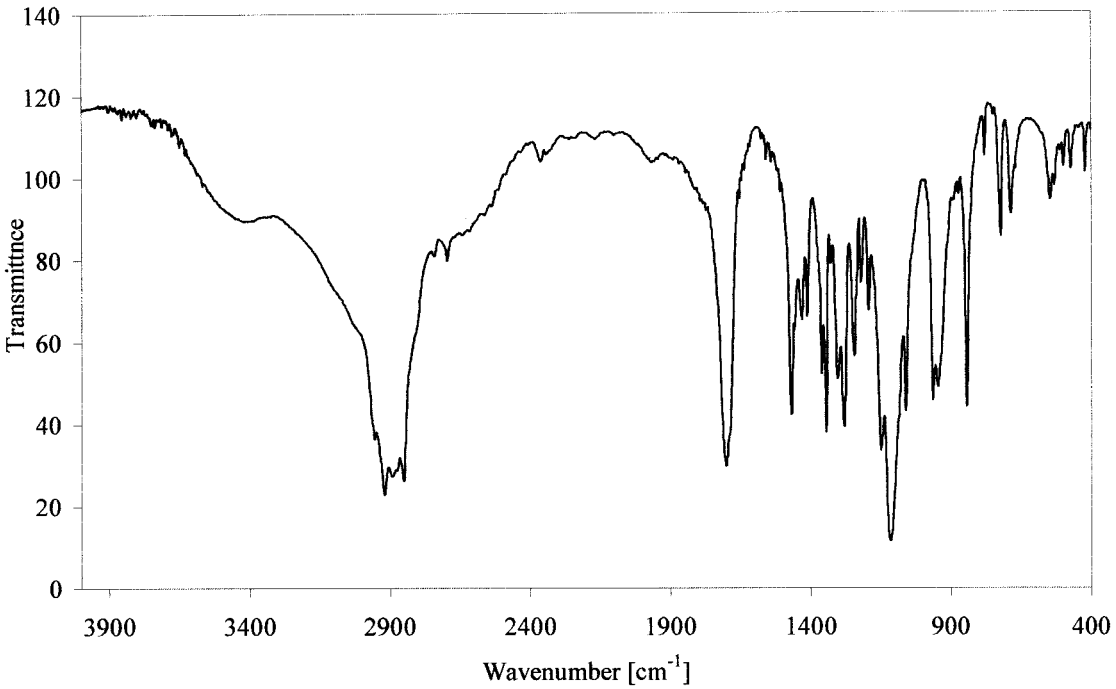

Figure 9 FTIR spectrum of a PEO/lauric acid blend.

structures and to attain desirable actuation in response to a stimulus with ferroelectrics, nonlinear optics, liquid crystals, and electrorheological fluids. Researchers have observed that the lamellar crystals within spherulites become aligned with the electric field because the induced polarization of the lamellae by the electric field is highest along the longest plane axis (PEO crystallizes as a 7/2 helix[34]).

For other polyethers, a more complex phase-transition behavior has been observed: during the heating of thermotropic polyethers synthesized from 1-(4-hydroxyphenyl)-2-(2-methyl-4-hydroxyphenyl)-

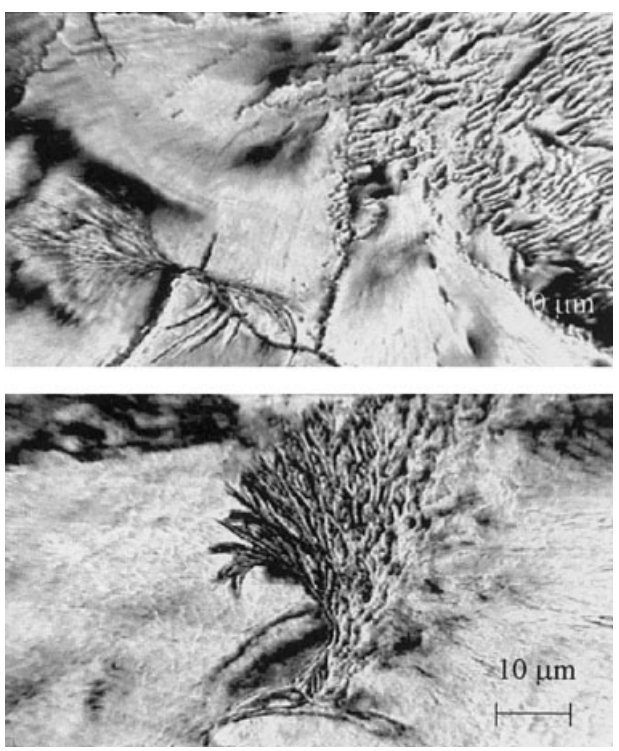

Figure 10 PLM micrographs of a PEO/lauric acid blend.

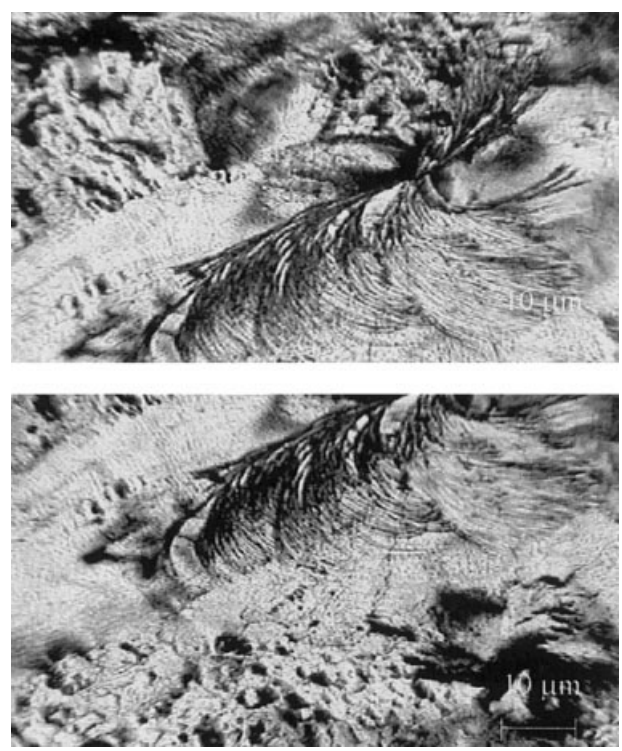

Figure 11 PLM micrographs of a PPO/lauric acid blend.

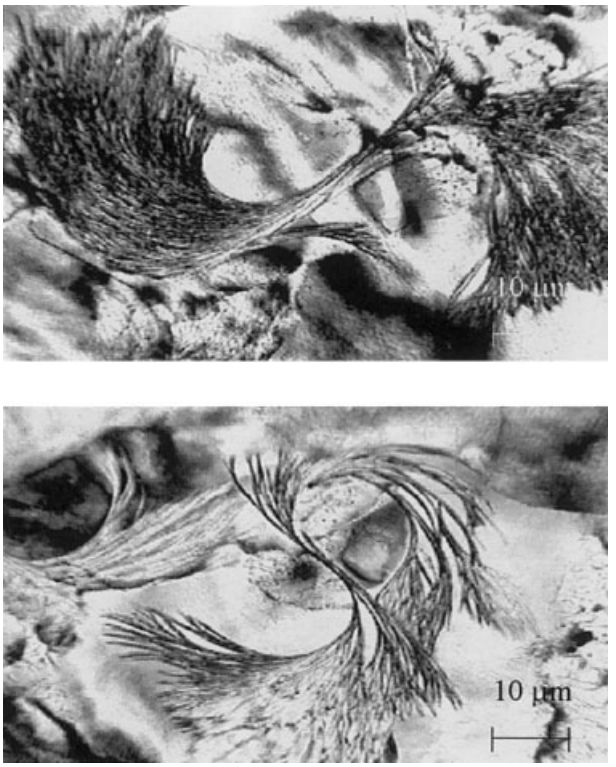

Figure 12 PLM micrographs of a PTHF/lauric acid blend.

ethane and α,ω-dibromo-*n*-alkanes with odd numbers of methylene units, and during successive heating, the heat of transition is a combination of the heat of fusion of the crystalline phase and the heat of isotropization of the mesophase region.[35] Researchers have discussed the mechanism responsible for the phase transitions in terms of structural, kinetic, and thermodynamic approaches that yield a description of the interfacial connections between crystalline and mesophase regions.

For the blends under investigation, hydrogen bonding plays an important role in facilitating the crystal formation. A study devoted solely to this important issue is currently underway.

CONCLUSIONS

Binary blends of PPO and PTHF with fatty acids show advantageous broader phase-transition ranges that are additionally shifted toward lower temperatures. PEO blends show not only this feature but also a synergistic effect, as evidenced by the heats of transition. This phenomenon may be explained in terms of the facilitated formation of hydrogen bonding between the hydrogen atom from the carboxylic group in acid molecules and the ether oxygen from the poly(oxyethylene) chain, as can be assumed from IR data. Hydrogen bonding enhances the formation of well-developed crystalline structures in the form of spherulites that gown with the spontaneous selection of the lamellar thickness. The textures of the individual fibrils, consisting of stacks of several tens of lamellae corresponding to PPO and PTHF, are less regular than the texture of PEO and show large macroscopic heterogeneity.

References

1. Encyclopedia of Polymer Science and Technology (online edition); Wiley: New York (accessed October 2002).
2. Miyano, W.; Inoue, E.; Tsuchiya, M.; Ishimaru, K.; Kojima, T. J Therm Anal Calorim 2001, 64, 459.
3. Armitstead, K.; Goldbeck-Wood, G. Adv Polym Sci 1992, 100, 219.
4. Frank, F. C.; Keller, A.; Mackley, M. R. Polymer 1971, 12, 46.
5. Muthukumar, M. Eur Phys J 2000, 3, 199.
6. Welch, P.; Muthukumar, M. Phys Rev Lett 2001, 87, 218302.
7. Sari, A.; Kaygusuz, K. Sol Energy 2001, 71, 365.
8. Banu, D.; Feldman, D.; Hawes, D. Thermochim Acta 1998, 317, 39.
9. Lisowski, M. S.; Liu, Q.; Cho, J.; Runt, J. Macromolecules 2000, 33, 4842.
10. Cheng, S. Z. D.; Wunderlich, B. J Polym Sci Part B: Polym Phys 1986, 24, 595.
11. Akalu, Y.; Kielhorn, L.; Hasio, B. S.; Stein, R. S.; Russell, T. P.; van Egmond, J.; Muthukumar, M. Macromolecules 1999, 32, 705.
12. Pielichowski, K.; Flejtuch, K. Polym Adv Technol 2002, 13, 1.
13. Pielichowski, K.; Flejtuch, K. Macromol Mater Eng 2002, 288, 259.
14. Jutier, J.; Lemieux, E.; Prud'homme, R. E. J Polym Sci Part B: Polym Phys 1988, 26, 1313.
15. Guo, Y.; Liang, X. J Macromol Sci Phys 1999, 38, 439.
16. Philippova, O. E.; Kuchanov, S. I.; Topchieva, I. N.; Kabanov, V. A. Macromolecules 1985, 18, 1628.
17. Haynes, C. A.; Beynon, R. A.; King, R. S.; Blanch, H.; Prausnitz, J. M. J Phys Chem 1989, 93, 5612.
18. Polik, W. F.; Burchard, W. Macromolecules 1983, 16, 978.
19. Economou, I. G.; Cui, Y.; Donohue, M. D. Macromolecules 1991, 24, 5058.
20. Bogdanov, B. G.; Michailov, M.; Uzov, C. V.; Gavrailova, G. G. J Polym Sci Part B: Polym Phys 1994, 32, 387.
21. Cesteros, L. C.; Rego, J. M.; Vazquez, J. J.; Katime, I. Polym Commun 1990, 31, 153.
22. Coleman, M. M.; Lee, J. Y.; Serman, C. J.; Wang, Z.; Painter, P. C. Polymer 1989, 30, 1298.
23. Kovacs, A. J.; Straupe, C. J Chem Soc Faraday Discuss 1979, 68, 225.
24. Kovacs, A. J.; Straupe, C. J Cryst Growth 1980, 48, 210.
25. Cheng, S. Z. D.; Chen, J.; Heberer, D. P. Polymer 1992, 33, 1429.
26. Cheng, S. Z. D.; Chen, J. H.; Zhang, A. Q.; Heberer, D. P. J Polym Sci Part B: Polym Phys 1991, 29, 299.
27. Cheng, S. Z. D.; Chen, J. H. J Polym Sci Part B: Polym Phys 1991, 29, 311.
28. Hoffman, J. D. Macromolecules 1986, 19, 1124.
29. Treatise on Solid State Chemistry; Hoffman, J. D.; Davis, G. T.; Lauritzen, J. I., Jr.; Hannay, N. B., Eds.; Plenum Press: New York, 1976; p 497.
30. Hoffman, J. D.; Miller, R. L. Macromolecules 1988, 21, 3038.
31. Ding, N.; Amis, E. J. Macromolecules 1991, 24, 3906.
32. Ishikiriyama, K.; Wunderlich, B. Macromolecules 1997, 30, 4126.
33. Park, C.; Robertson, R. E. Polymer 2001, 42, 2597.
34. Bailey, F. E., Jr.; Koleske, J. V. Polyethylene Oxide; Academic Press: London, 1976.
35. Yandrasits, M. A.; Chen, J.; Arnold, F. E., Jr.; Cheng, S. Z. D. Polym Adv Technol 1994, 5, 775.